Inorg. Chem. **2003**, *42*, 3340–3346

Low-Valent Cobalt Complexes with Three Different π Acceptor Ligands: Experimental and DFT Studies of the Reduced and the Low-Lying Excited States of (R-DAB)Co(NO)(CO), R-DAB = Substituted 1,4-Diaza-1,4-butadiene

Monika Sieger,[†] Matthias Wanner,[†] Wolfgang Kaim,*[,†] Derk J. Stufkens,[‡] Theo L. Snoeck,[‡] and Stanislav Záliš[§]

Institut für Anorganische Chemie, Universität Stuttgart, Pfaffenwaldring 55, D-70550 Stuttgart, Germany, Institute of Molecular Chemistry, Universiteit van Amsterdam, Nieuwe Achtergracht 166, 1018 WV Amsterdam, The Netherlands, and J. Heyrovský Institute of Physical Chemistry, Academy of Sciences of the Czech Republic, Dolejškova 3, CZ-18223 Prague, Czech Republic

Received October 2, 2002

The complexes (RN═CH—CH═NR)Co(NO)(CO) with R = isopropyl, 2,6-diisopropylphenyl, or *p*-tolyl are chemically and electrochemically reducible to radical anions at potentials which strongly depend on R. The DFT calculated structure for the neutral compound with R = *i*Pr agrees with the experiment, and the computed structure of the anion radical reveals changes according to a reduction of the R-DAB ligand. EPR results confirm an (R-DAB)-based singly occupied molecular orbital in $[(RNCHCHNR)Co(NO)(CO)]^{\bullet-}$, with minor but detectable contributions from NO as supported by IR spectroelectrochemistry and as quantified by DFT spin density calculations. The calculations indicate increasingly stabilized CO, NO, and RNCHCHNR π^* acceptor orbitals, in that order. On the basis of TD-DFT (time-dependent density functional theory) calculations, the lowest-lying excited states are assigned to metal-to-(R-DAB) charge transfer transitions while bands due to the metal-to-nitrosyl charge transfer occur at higher energies but still in the visible region. Resonance Raman studies were used to probe these assignments.

1,4-Disubstituted 1,4-diaza-1,3-butadienes (R-DAB) are unique chelate ligands[1] with a recognized potential in catalysis.[2] Their capability to stabilize metal centers in low oxidation states[1,3,4] is a consequence of low-lying π^* orbitals. Occupation of these orbitals can occur (i) through metal-to-ligand, ligand-to-ligand, or σ-bond-to-ligand charge transfer (MLCT, LLCT, or SBLCT) (eq 1a,b) in excited states, causing light absorption and color of many such compounds,[5] (ii) through chemical or electrochemical external electron transfer (eq 2) which leads to EPR-detectable anion radical complexes,[6] or (iii) through intramolecular electron transfer in the ground state (eq 3) which is evident, e.g., from structural effects, viz., a lengthening of the CN bonds and a shortening of the C^2C^3 bond of coordinated R-DAB.[7] For instance, the crystal structure of (RNCHCHNR)Ir(η^5-C_5Me_5), R = 2,6-dimethylphenyl, has shown that the ligand exists as a dianion $(RN—CH═CH—NR)^{2-}$ with iridium(III) as

* Corresponding author. E-mail: kaim@iac.uni-stuttgart.de.
† Institut für Anorganische Chemie.
‡ Institute of Molecular Chemistry.
§ J. Heyrovsky Institute.

(1) van Koten, G.; Vrieze, K. *Adv. Organomet. Chem.* **1982**, *21*, 151 and references therein.
(2) (a) Johnson, L. K.; Kilian, C. M.; Brookhart, M. *J. Am. Chem. Soc.* **1995**, *117*, 6414. (b) Johnson, L. K.; Mecking, S.; Brookhart, M. *J. Am. Chem. Soc.* **1996**, *118*, 267. (c) Schleis, T.; Spaniol, T. P.; Okuda, J.; Heinemann, J.; Mülhaupt, R. *J. Organomet. Chem.* **1998**, *569*, 159. (d) Gibson, V. C.; O'Reilly, R. K.; Reed, W.; Wass, D. F.; White, A. J. P.; Williams, D. J. *Chem. Commun.* **2002**, 1850.
(3) Bock, H.; tom Dieck, H. *Angew. Chem.* **1966**, *78*, 549; *Angew. Chem., Int. Ed. Engl.* **1966**, *5*, 520.
(4) tom Dieck, H.; Franz, K.-D.; Hohmann, F. *Chem. Ber.* **1975**, *108*, 163.
(5) (a) Servaas, P. C.; Stufkens, D. J.; Oskam, A. *Inorg. Chem.* **1989**, *28*, 1774. (b) Servaas, P. C.; Stufkens, D. J.; Oskam, A. *Inorg. Chem.* **1989**, *28*, 1780.
(6) (a) Franz, K.-D.; tom Dieck, H.; Krynitz, U.; Renk, I. W. *J. Organomet. Chem.* **1974**, *64*, 361. (b) Andrea, R. R.; de Lange, W. G. J.; van der Graf, T.; Rijkhoff, M.; Stufkens, D. J.; Oskam, A. *Organometallics* **1988**, *7*, 1100.
(7) Greulich, S.; Kaim, W.; Stange, A.; Stoll, H.; Fiedler, J.; Zalis, S. *Inorg. Chem.* **1996**, *35*, 3998.

10.1021/ic026078t CCC: $25.00
Published on Web 04/25/2003

coordinated metal center.[7]

$$(\text{R-DAB})\text{M}^k\text{L}_n \xrightarrow[\text{MLCT}]{h\nu} [(\text{R-DAB}^{\text{I}-})\text{M}^{k+1}\text{L}_n]^* \quad (1a)$$

$$(\text{R-DAB})\text{ML}_n \xrightarrow[\text{LLCT}]{h\nu} [(\text{R-DAB}^{\text{I}-})\text{ML}_{n-1}\text{L}^{\text{I}+}]^* \quad (1b)$$

$$(\text{R-DAB})\text{M}^k\text{L}_n \underset{-e^-}{\overset{+e^-}{\rightleftharpoons}} [(\text{R-DAB}^{\text{I}-})\text{M}^k\text{L}_n]^{\bullet -} \quad (2)$$

$$(\text{R-DAB})\text{M}^k\text{L}_n \leftrightarrow [(\text{R-DAB}^{\text{II}-})\text{M}^{k+2}\text{L}_n] \quad (3)$$

We have previously studied several complexes of the R-DAB ligands with small organometallic groups ML_n such as $PtMe_2$, $PtMe_4$,[8] ZnR_2,[9] $[Ir(\eta^5\text{-}C_5Me_5)Cl]^+$, or $Ir(\eta^5\text{-}C_5Me_5)$,[7] both experimentally (structure, electrochemistry, spectroscopy) and theoretically (ab initio methods). The symmetry and small size of the R-DAB ligands and of the aforementioned ML_n complex fragments allowed us to obtain fairly clear pictures of the electronic structures which could serve as starting points for discussions of reactivity.[8−10]

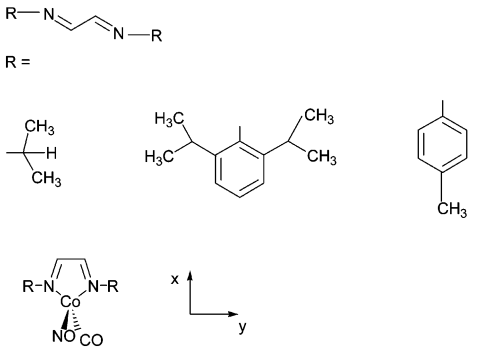

In the following, we describe experimental and computational studies of the reduced and low-lying excited states of the compounds (RNCHCHNR)Co(NO)(CO), R = isopropyl (*i*Pr), 2,6-diisopropylphenyl (Dipp), or *p*-tolyl (*p*-Tol).[11] Whereas the carbonylmetal complexes of the α-diimine ligands have been extensively investigated for more than 30 years,[3] there were few reports on nitrosylmetal-containing compounds.[12−14] The recent biochemically motivated interest in NO coordination chemistry[15,16] has led us

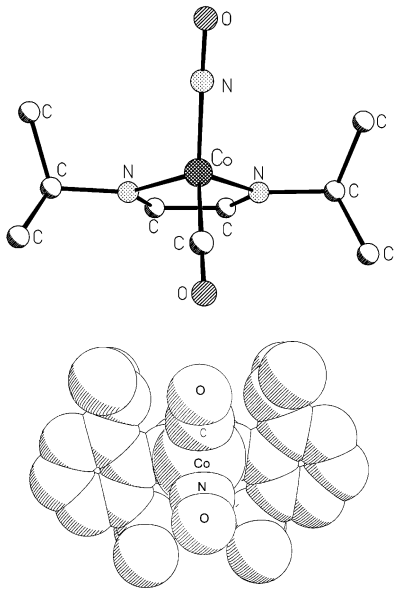

Figure 1. Molecular structure of (*i*Pr-DAB)Co(NO)(CO) (top) and space-filling representation of the molecular structure of (Dipp-DAB)Co(NO)(CO) (bottom).

to consider mixed NO/CO metal complexes for detailed studies despite the crystallographic problems of NO/CO disorder.[11] Following a re-examination of highly labile (bpy)Co(NO)(CO),[13] we present the electrochemical, spectroscopic (EPR), and IR-spectroelectrochemical characterization of the systems $[(\text{RNCHCHNR})\text{Co(NO)(CO)}]^{0/-}$. DFT calculations on the species with R = *i*Pr (for which the ground state structure is known, Figure 1)[11] and R = Me were employed to elucidate the electronic structure, including the sequence of RNCHCHNR, NO, and CO π^* acceptor orbitals. Time-dependent density functional theory (TD-DFT) methodology[17] was then applied to assign the low-energy absorption features, especially with respect to the role of the NO ligand; resonance Raman (rR) studies were employed to further investigate these absorptions.

Experimental Section

Instrumentation. EPR spectra were recorded in the X-band on a Bruker System ESP 300 equipped with a Bruker ER035M gaussmeter and a HP 5350B microwave counter. Infrared spectra were obtained using a Perkin-Elmer Paragon 1000 PC FTIR instrument. UV−vis−NIR absorption spectra were recorded on a Bruins Instruments Omega 10 spectrophotometer. Cyclic voltammetry was carried out at 100 mV/s scan rate in acetonitrile/0.1 M Bu_4NPF_6 using a three-electrode configuration (glassy carbon working electrode, Pt counter electrode, Ag/AgCl reference) and a PAR 273 potentiostat and function generator. The ferrocene/ferrocenium couple served as internal reference. IR-spectroelectrochemical measurements were performed using an optically transparent thin-layer electrode (OTTLE) cell.[19] EPR spectra were measured best from THF solutions in which the radical anion complexes were generated by reduction with K in the presence of K^+-encapsulating [2.2.2] cryptand.[20] Resonance Raman spectra were

(8) (a) Hasenzahl, S.; Hausen, H.-D.; Kaim, W. *Chem. Eur. J.* **1995**, *1*, 95. (b) Klein, A.; Hasenzahl, S.; Kaim, W. *J. Chem. Soc., Perkin Trans. 2* **1997**, 2573. (c) Kaim, W.; Klein, A.; Hasenzahl, S.; Stoll, H.; Zalis, S.; Fiedler, J. *Organometallics* **1998**, *17*, 237. (d) van Slageren, J.; Klein, A.; Zalis, S. *Coord. Chem. Rev.* **2002**, *230*, 193.

(9) Kaupp, M.; Stoll, H.; Preuss, H.; Kaim, W.; Stahl, T.; van Koten, G.; Wissing, E.; Smeets, W. J. J.; Spek, A. L. *J. Am. Chem. Soc.* **1991**, *113*, 5606.

(10) (a) Berger, S.; Baumann, F.; Scheiring, T.; Kaim, W. *Z. Anorg. Allg. Chem.* **2001**, *627*, 620. (b) Greulich, S.; Klein, A.; Knoedler, A.; Kaim, W. *Organometallics* **2002**, *21*, 765.

(11) Sieger, M.; Hübler, K.; Scheiring, T.; Sixt, T.; Zalis, S.; Kaim, W. *Z. Anorg. Allg. Chem.*, **2002**, *628*, 2360.

(12) tom Dieck, H.; Haarich, M. *J. Organomet. Chem.* **1985**, *291*, 71.

(13) Brunner, H.; Faustmann, P.; Dietl, A.; Nuber, B. *J. Organomet. Chem.* **1997**, *542*, 255.

(14) tom Dieck, H.; Bruder, H.; Kühl, E.; Junghans, D.; Hellfeldt, K. *New J. Chem.* **1989**, *13*, 259.

(15) (a) *Methods in Nitric Oxide Research*; Feelisch, M., Stamler, J. S., Eds.; Wiley: Chichester, U.K., 1996. (b) Murat, F. *Angew. Chem.* **1999**, *111*, 1976; *Angew. Chem., Int. Ed. Engl.* **1989**, *28*, 1856. (c) Richter-Addo, G. B.; Legzdins, P.; Burstyn, J. *Chem. Rev.* **2002**, *102*, 857.

(16) (a) Wolak, M.; van Eldik, R. *Coord. Chem. Rev.* **2002**, *230*, 263. (b) Baraldo, L. M.; Forlano, P.; Parise, A. R.; Slep, L. D.; Olabe, J. A. *Coord. Chem. Rev.* **2001**, *219−221*, 881.

(17) Gross, E. K. U.; Dobson, J. F.; Petersilka, M. *Top. Curr. Chem.* **1996**, *181*, 81.

obtained for KNO_3 pellets by excitation with two laser lines, 514.5 nm (SP 2016 argon ion laser) or 605 nm (Rhodamine 6G dye laser line, pumped by the argon ion laser). The spectra were recorded by a Dilor XY spectrometer.

The syntheses of the complexes and the crystallographic characterization of **1** and **2** have been described.[11,13]

Quantum-Chemical Calculations. Calculations of (R-DAB)Co(NO)(CO) complexes (R = alkyl) in the ground state (R = *i*Pr) and in the reduced state (R = Me) have been done by density functional theory (DFT) methods using the Gaussian 98[21] and Amsterdam Density Functional (ADF2000.02[22,23]) program packages.

B3LYP hybrid functionals[24] were used within Gaussian 98 (G98/B3LYP). The cobalt valence double-ζ plus polarization basis set designed for DFT calculations was taken from Godbout et al.[25] while Dunning's[26] valence double-ζ with polarization functions were used for C, N, and H atoms within geometry optimization and calculations of vibrational frequencies (basis I). An augmented double-ζ atomic natural orbital basis[27] (ANO-contraction (21s,15p,10d,6f) → [6s,5p,4d,2f]) for cobalt together with the EPR-II basis[28] for C, N, and H atoms (basis II) were used to calculate the spin distribution and Fermi contact terms.

Within the ADF program, Slater type orbital (STO) basis sets of triple-ζ quality with polarization functions for C, N, O, and Co atoms were employed. Inner shells were represented by the frozen core approximation (1s for C, N, and O, 1s−3p for Co were kept frozen). Core electrons were included for calculating the spin distribution and **A** matrices. Within ADF, the functional including Becke's gradient correction to the local exchange expression in conjunction with Perdew's gradient correction to local density approximation (LDA) with VWN parametrization of electron gas data was used (ADF/BP).[29,30] The lowest excited states of closed shell complexes were calculated using the time-dependent DFT (TD-DFT) method.[17] IR frequencies were calculated at optimized geometries.

The calculations were performed within the constraints of C_s symmetry, the *xy* plane of symmetry coinciding with the C(CO)−Co−N(NO) plane. A spin-unrestricted Kohn−Sham formalism was used for the radical anions $[(Me\text{-}DAB)Co(NO)(CO)]^{\bullet-}$.

Table 1. Electrochemical and Spectroscopic Data of Complexes (R-DAB)Co(NO)(CO)

	R		
	*i*Pr	Dipp	*p*-Tol
	Redox Potentials[a]		
$E_{1/2}$(red1)	−2.00	−1.58	−1.36
$E_{1/2}$(red2)	n.o.	n.o.	−2.01
E_{pa}(ox1)	−0.38	−0.04	−0.24
	Absorption Maxima[b]		
λ_{max}	545	573	621
	438	432sh	388
	330sh		
	Stretching Vibrations[c]		
ν_{CO}(0)	1942	1962	1957
($^{\bullet-}$)	1868	1882	1890
ν_{NO}(0)	1689	1712	1703
($^{\bullet-}$)	1577	1604	1599
	EPR Data[d]		
g	1.9937	1.9970	2.0012
$A(^{59}Co)$	1.13	1.53	1.84
$A(^{14}N)$, R-DAB	0.65	0.705	n.o.
$A(^{14}N)$, NO	0.22	0.335	n.o.
$A(^{1}H)$	0.41	0.385	n.o.

[a] In CH_3CH/0.1 M Bu_4NPF_6 at 100 mV/s scan rate; potentials vs $[Fe(C_5H_5)_2]^{+/0}$. E_{pa} = anodic peak potential; n.o. = not observed. [b] In toluene. [c] In acetonitrile. [d] In THF/[2.2.2] cryptand.

Experimental Results and Discussion

The complexes (RNCHCHNR)Co(NO)(CO) are obtained as air-sensitive, colored substances from the reaction of $Co(CO)_3(NO)$ with the corresponding R-DAB ligands *i*Pr-DAB, Dipp-DAB,[31] and *p*-Tol-DAB. The air-sensitivity decreases in the series (bpy)Co(NO)(CO), (R-DAB)Co(NO)(CO), R = *i*Pr, *p*-Tol, Dipp; the Dipp-DAB complex is shielded from external attack by the bulky substituents (Figure 1).

All complexes could be reversibly reduced in acetonitrile solution. The potentials for that one-electron process as listed in Table 1 reveal that the *p*-Tol-DAB complex is easiest to reduce whereas the *i*Pr-DAB complex has a rather negative reduction potential, in agreement with established substituent effects of R. The complex with R = *p*-Tol could be reduced quasireversibly to a dianion. With −1.75 V, the reduction potential of the highly sensitive (bpy)Co(NO)(CO) lies between that of (*i*Pr-DAB)Co(NO)(CO) and those of the R-DAB complexes with aromatic R. Oxidation occurs at rather low potentials but is always irreversible, presumably due to loss of the CO ligand.

A typical absorption spectrum of the R-DAB complexes is shown in Figure 2; in Table 1, the slightly solvent-dependent[11] absorption data are summarized together with other experimental results. In each case, there are two discernible absorption bands in the visible and the near UV regions.

(18) (a) van Slageren, J.; Klein, A.; Zalis, S.; Stufkens, D. J. *Coord. Chem. Rev.* **2001**, *219*−*221*, 937. (b) Servaas, P. C.; van Dijk, H. K.; Snoeck, T. L.; Stufkens, D. J.; Oskam, A. *Inorg. Chem.* **1985**, *24*, 4494. (c) Balk, R. W.; Stufkens, D. J.; Oskam, A. *J. Chem. Soc., Dalton Trans.* **1981**, 1124.

(19) Krejcik, M.; Danek, M.; Hartl, F. *J. Electroanal. Chem.* **1991**, *317*, 179.

(20) Waldhör, E.; Kaim, W.; Olabe, J. A.; Slep, L. D.; Fiedler, J. *Inorg. Chem.* **1997**, *36*, 2969.

(21) Frisch, M. J.; Trucks, G. W.; Schlegel, H. B.; Scuseria, G. E.; Robb, M. A.; Cheeseman, J. R.; Zakrzewski, V. G.; Montgomery, J. A., Jr.; Stratmann, R. E.; Burant, J. C.; Dapprich, S.; Millam, J. M.; Daniels, A. D.; Kudin, K. N.; Strain, M. C.; Farkas, O.; Tomasi, J.; Barone, V.; Cossi, M.; Cammi, R.; Mennucci, B.; Pomelli, C.; Adamo, C.; Clifford, S.; Ochterski, J.; Petersson, G. A.; Ayala, P. Y.; Cui, Q.; Morokuma, K.; Malick, D. K.; Rabuck, A. D.; Raghavachari, K.; Foresman, J. B.; Cioslowski, J.; Ortiz, J. V.; Stefanov, B. B.; Liu, G.; Liashenko, A.; Piskorz, P.; Komaromi, I.; Gomperts, R.; Martin, R. L.; Fox, D. J.; Keith, T.; Al-Laham, M. A.; Peng, C. Y.; Nanayakkara, A.; Gonzalez, C.; Challacombe, M.; Gill, P. M. W.; Johnson, B. G.; Chen, W.; Wong, M. W.; Andres, J. L.; Head-Gordon, M.; Replogle, E. S.; Pople, J. A. *Gaussian 98*, revision A.7; Gaussian, Inc.: Pittsburgh, PA, 1998.

(22) Fonseca Guerra, C.; Snijders, J. G.; te Velde, G.; Baerends, E. J. *Theor. Chim. Acta* **1998**, *99*, 391.

(23) van Gisbergen, S. J. A.; Snijders, J. G.; Baerends, E. J. *Comput. Phys. Commun.* **1999**, *118*, 119.

(24) Stephens, P. J.; Devlin, F. J.; Cabalowski, C. F.; Frisch, M. J. *J. Phys. Chem.* **1994**, *98*, 1162.

(25) Godbout, N.; Salahub, D. R.; Andzelm, J.; Wimmer, E. *Can. J. Chem.* **1992**, *70*, 560.

(26) Pou-Amerigo, R.; Merchan, M.; Nebot-Gil, I.; Widmark, P. O.; Roos, B. *Theor. Chim. Acta* **1995**, *92*, 149.

(27) Woon, D. E.; Dunning, T. H., Jr. *J. Chem. Phys.* **1993**, *98*, 1358.

(28) Barone, V. In *Recent Advances in Density Functional Methods, Part I*; Chong, D. P., Ed.; World Scientific: Singapore, 1996.

(29) Becke, A. D. *Phys. Rev. A* **1988**, *38*, 3098.

(30) Perdew, J. P. *Phys. Rev. A* **1986**, *33*, 8822.

(31) Berger, S.; Baumann, F.; Scheiring, T.; Kaim, W. *Z. Anorg. Allg. Chem.* **2001**, *627*, 620.

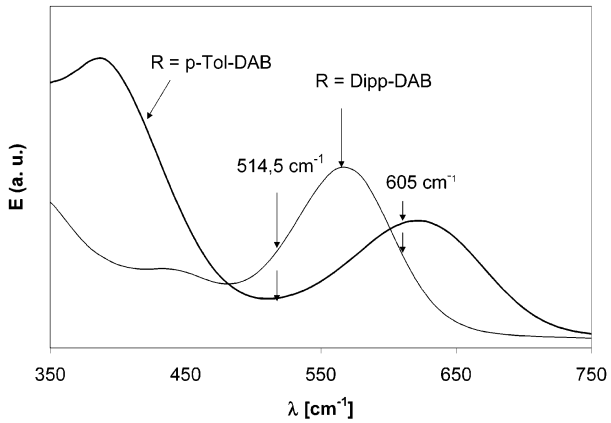

Figure 2. Absorption spectra of (*p*-Tol-DAB)Co(NO)(CO) and (Dipp-DAB)Co(NO)(CO) in toluene with positions of rR excitation wavelengths.

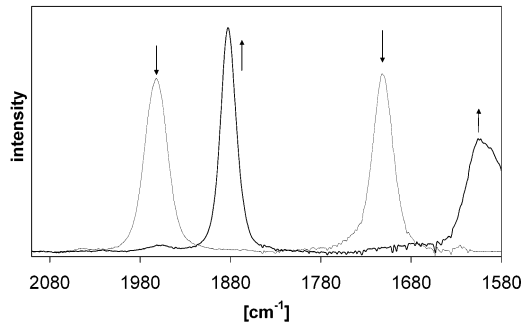

Figure 3. IR-spectroelectrochemistry of the transition [(Dipp-DAB)Co(NO)(CO)]$^{(0)\rightarrow(-)}$ in CH_3CN/0.1 M Bu_4NPF_6.

To investigate the possible contributions from the NO and CO acceptor ligands in the singly occupied MO, we studied the shifts of the CO and NO stretching bands by IR-spectroelectrochemistry, using an optically transparent thin-layer electrolytic (OTTLE) cell.[19] In agreement with DFT calculation results (see later), the experiments as illustrated by Figure 3 show a smaller shift for ν(CO) than for ν(NO) during the transitions [(RNCHCHNR)Co(NO)(CO)]$^{0/\bullet-}$ (Table 1); however, the ca. 110 cm^{-1} low-energy shifts for ν(NO) are still small in comparison to the ca. 300 cm^{-1} shifts observed in the course of the nitrosyl-based reductions $[(NC)_5M^{II}(NO^+)]^{2-} \rightarrow [(NC)_5M^{II}(NO^\bullet)]^{3-}$, M = Ru or Os.[32]

Nevertheless, the charge effect alone can obviously cause sizable shifts in the absence of significant electron delocalization to a ligand like CO; similar such effects were noted before.[33]

Reliable information on the distribution of the unpaired electron comes from EPR spectroscopy of the anion radical complexes [(RNCHCHNR)Co(NO)(CO)]$^{\bullet-}$. Several complexes (R-DAB$^{\bullet-}$)ML$_n$ have been studied by high-resolution EPR (Table 2);[8b] the spectra of the systems described here have additional hyperfine splitting from the metal (^{59}Co: $I = {}^7/_2$) and from NO (^{14}N: $I = 1$), as illustrated in Figure 4 and as quantified in Tables 1 and 2.

Despite the domination of the EPR spectra by the quite variable ^{59}Co hyperfine splitting and the complexity added by ^{1}H and ^{14}N couplings from the R-DAB ligand, it was also possible to establish the ^{14}N splitting from the nitrosyl ligand in two instances, in agreement with previous data for related systems (Table 2) and with calculations (cf. discussion in later paragraphs). In the series of radical complexes (R-DAB$^{\bullet-}$)ML$_n$ from Table 2, an increasing NO and decreasing CO content corresponds to a decreasing ^{14}N hyperfine coupling of the R-DAB ligand, signifying more spin delocalization from (R-DAB)$^{\bullet-}$ to the nitrosyl than to the carbonyl ligand.

A special effect of the NO acceptor ligand is also evident from the atypical *g* factors, *g*(complex) < *g*(electron) = 2.0023, which indicate additional excited states (involving π^*_{NO}) with nonzero angular momentum lying close to the doublet ground state.[34] Both the isotropic *g* value and

Table 2. EPR Data of 1,4-Diazabutadiene Radical Complexes [(R-DAB)ML$_n$]$^{\bullet-}$[a]

ML$_n$	a(^{1}H)/mT	a(^{14}N)/mT	a(M)/mT	a(M)/10^{-3} A_{iso}
Re(CO)$_3^{+}$ [b]	0.465	0.726	3.561 (^{185,187}Re)	11.05
Mn(CO)$_3^{+}$ [b]	0.435	0.748	0.847 (^{55}Mn)	7.75
Mo(CO)$_4$ [c]	0.42	0.707	0.29 (^{95,97}Mo)	6.16
Co(NO)(CO)	0.41	0.65	1.13 (^{59}Co) [f]	7.21
Fe(NO)$_2$ [e]	0.425	0.575	n.o.[g]	

[a] Coupling constants a in mT, isotropic coupling constants A_{iso} from ref 37; R = *t*Bu except for ML$_n$ = Co(NO)(CO). [b] In benzene or toluene (ref 6b). [c] In 1,2-dimethoxyethane (ref 6a). [d] In THF (this work), R = *i*Pr. [e] In 1,2-dimethoxyethane (ref 14). [f] a(^{14}N) = 0.22 mT (1 NO). [g] a(^{14}N) = 0.155 mT (2 NO).

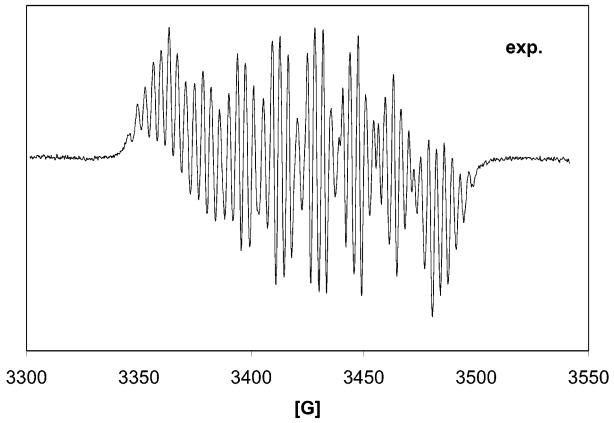

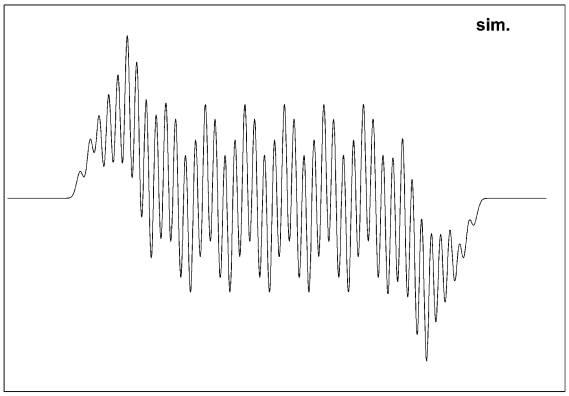

Figure 4. ESR spectrum of [(Dipp-DAB)Co(NO)(CO)]$^{\bullet-}$ in THF solution (top) with computer simulation (bottom).

(32) Baumann, F.; Kaim, W.; Baraldo, L. M.; Slep, L. D.; Olabe, J. A.; Fiedler, J. *Inorg. Chim. Acta* **1999**, *285*, 129.
(33) Kaim, W.; Bruns, W.; Kohlmann, S.; Krejcik, M. *Inorg. Chim. Acta* **1995**, *229*, 143.
(34) Kaim, W. *Coord. Chem. Rev.* **1987**, *76*, 187.

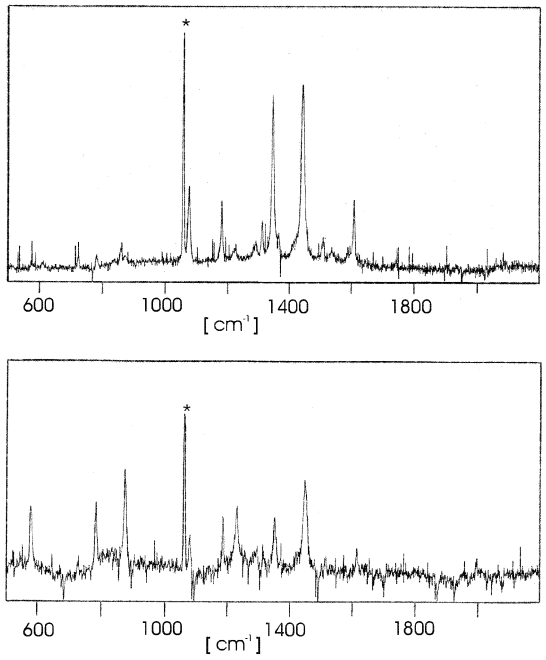

Figure 5. Resonance Raman spectra of (*p*-Tol-DAB)Co(NO)(CO) in KNO_3 (∗) obtained by excitation with 514.5 nm (top) and 605 nm wavelength (bottom).

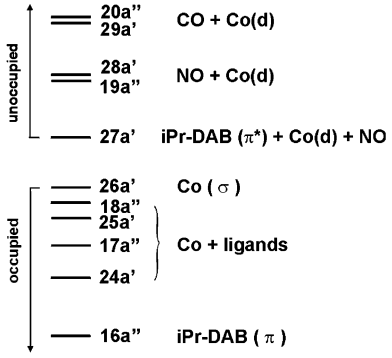

Figure 6. Qualitative molecular orbital scheme for [(*i*Pr-DAB)Co(NO)(CO)] calculated by the ADF method.

$a(^{59}Co)$ increase on going from alkyl- to aryl-substituted species, in agreement with better π accepting R-DAB ligation and diminishing contributions from NO.

Resonance Raman spectra could be obtained for (*p*-Tol-DAB)Co(NO)(CO) and (Dipp-DAB)Co(NO)(CO) at selected wavelengths in the visible region (Figure 5). Photodecomposition set in at higher energies of irradiation while the complex (*i*Pr-DAB)Co(NO)(CO) proved to be too sensitive altogether for rR studies. The resonance Raman spectra of (*p*-Tol-DAB)Co(NO)(CO) are rather intense, and the band pattern depends on the wavelength of excitation. At 514.5 nm excitation, the only rR effects are observed for stretching modes of the *p*-Tol-DAB ligand in the 1000−1650 cm^{-1} region, whereas at 605 nm excitation, both the stretching and deformation modes of the *p*-Tol-DAB ligand and possibly metal−ligand stretching and M−C(N)−O deformation modes are resonance enhanced in the region below 1000 cm^{-1}. Both spectra do not show any rR effect for ν(CO) and ν(NO).

This result indicates that there are two MLCT transitions to the *p*-Tol-DAB ligand within the broad absorption band with clearly different charge transfer character. Excitation at 514.5 nm takes place into an MLCT transition which has much CT character since the main rR effects are observed for the ligand stretching modes. At 605 nm, the excitation involves a transition which has much less CT character and is thus likely to occur between those orbitals which are responsible for the metal-to-ligand π back-bonding. This π back-bonding is in fact a mixing between the metal d_π and R-DAB ligand π^* orbitals, and because of this mixing, the transition between these orbitals obtains less charge transfer and more metal−ligand bonding-to-antibonding character. In the extreme case of complete 1:1 mixing, the transition would have no charge-transfer character at all which is then manifested by the disappearance from the rR spectra of the ligand stretching vibrations.[18] Transitions having some metal−ligand bonding-to-antibonding character normally show increased resonance enhancement of metal−ligand stretching and ligand deformation modes since in a metal−ligand antibonding excited state the metal−ligand bonds are weakened and the ligand is distorted. Varying degrees of metal-to-diimine π back-bonding and MLCT transitions with different CT character have been studied by rR spectroscopy under both metal[18b] and ligand variation.[18c]

The rR spectra obtained for (Dipp-DAB)Co(NO)(CO) are much weaker than those for the *p*-Tol-DAB analogue. Both spectra show rR effects for ligand stretching as well as metal−ligand stretching and ligand deformation modes. Again, the excitation at the two different wavelengths involves transitions having different CT character, but the difference is not as clear as for the *p*-Tol-DAB complex. The transition at 514.5 nm seems to have more CT character than the transition at 605 nm, since the relative intensities of the metal−ligand stretching and ligand deformation modes are somewhat lower in the 514.5 nm excited spectrum.

DFT Calculations and Discussion

Geometry-optimized DFT calculations of [(R-DAB)Co(NO)(CO)]^n, R = *i*Pr (n = 0) or Me (n = 1−), not only confirm the ground state geometries[11] but also indicate the effect of the electron acquisition (Table 4): The most pronounced effects are a lengthening of the CN(imine) bonds, a shortening of the C^2C^3 bond of R-DAB, and a lengthening of the Co−N(imine) bonds. These results point to a predominant reduction of the R-DAB ligand;[7] the effects in the Co−NO and Co−CO bonds are marginal by comparison. Calculated selected bond lengths and angles are listed in Table 4. Both the ADF/BP and G98/B3LYP calculated geometries of **1** are in good agreement with the experimental structure.

The qualitative MO scheme of (*i*Pr-DAB)Co(NO)(CO) as calculated by ADF/BP is depicted in Figure 6; the analysis of virtual orbitals is listed in Table 3. The highest occupied MO (HOMO), 26a′, is mainly localized on the central metal atom. The central metal atom contributes more than 50% to the set of lower-lying occupied orbitals 18a″ and 25a′; these orbitals are to some extent delocalized over the ligand sphere. Together with 17a″ and 24a″, these five highest occupied

Table 3. Resonance Raman Enhanced Frequencies (cm^{-1}) at 514.5 nm Excitation

(Dipp-DAB)Co-(NO)(CO)	(*p*-Tol- DAB)Co-(NO)(CO)
335	568
592	776
701	867
860	1070
929	1174
1152	1222
1189	1285
1245	1309
1436	1340
1449	1438
1586	1505
1640	1604

Table 4. Selected Experimental Bond Lengths (Å) and Angles (deg) of (*i*Pr-DAB)Co(NO)(CO) and Calculated Values for [(Me-DAB)Co(NO)(CO)]$^{\bullet-}$ [a]

	(*i*Pr-DAB)Co(NO)(CO)			[(Me-DAB)Co(NO)(CO)]$^{\bullet-}$	
bond lengths, angles	exptl[b]	calcd G98/B3LYP	calcd ADF/BP	calcd G98/B3LYP	calcd ADF/BP
Co−N (DAB)	1.956	1.948	1.962	2.009	2.025
Co−N (NO)	1.625	1.637	1.647	1.652	1.690
Co−C (CO)	1.773	1.757	1.771	1.729	1.745
N^1-C^2	1.296	1.325	1.314	1.344	1.342
C^2-C^3	1.433	1.437	1.426	1.407	1.403
N^1−C (R)	1.440	1.490	1.470	1.443	1.455
C−O	1.123	1.184	1.166	1.182	1.186
N−O	1.207	1.224	1.187	1.215	1.218
N^1-Co-N^4	79.6	82.1	81.0	80.6	79.7
$Co-N^1-C^2$	115.4	113.8	114.7	113.4	113.7
$N^1-C^2-C^3$	114.4	115.1	114.9	116.3	116.4
N(O)−Co−C(O)	110.2	107.9	107.8	109.3	109.8
Co−N−O	169.0	173.2	173.3	159.2	157.5
Co−C−O	179.3	177.6	177.7	178.5	178.5

[a] Optimized for [(Me-DAB)Co(NO)(CO)]$^{\bullet-}$, for [(*i*Pr-DAB)Co(NO)(CO)]$^{\bullet-}$ the optimization did not converge. [b] Averaged values.

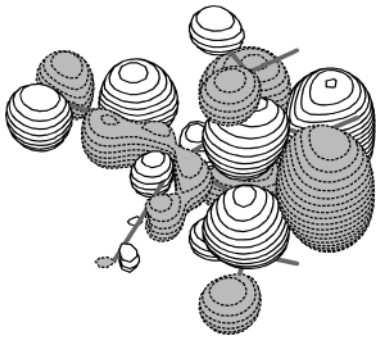

Figure 7. Molecular orbital representation for the SOMO of [(Me-DAB)-Co(NO)(CO)]$^{\bullet-}$ from DFT calculations (ADF). The NO group is located in upper left part of the picture.

MOs correspond to the filled $3d^{10}$ shell of cobalt(I−) in a distorted tetrahedral environment. The lowest-lying unoccupied MO (LUMO), 27a′, is mainly formed by the π^* orbital of *i*Pr-DAB ligand with contributing 3d metal and NO ligand orbitals (cf. Table 5). The following higher-lying unoccupied MOs 19a″ and 28a′ are formed by NO orbitals with some d_{Co} contribution. These near degenerate NO-based unoccupied orbitals are then followed by the CO-based molecular orbitals 29a′ and 20a″.

During the reduction process, an electron is accepted by the LUMO 27a′ which becomes a singly occupied MO (SOMO); this orbital is depicted in Figure 7.

Table 5. ADF/BP Calculated One-Electron Energies and Percentage Composition of Highest Occupied and Lowest Unoccupied Molecular Orbitals of (*i*Pr-DAB)Co(NO)(CO), Expressed in Terms of Composing Fragments

MO	*E* (eV)	prevailing character	Co	NO	CO	*i*Pr-DAB
			Unoccupied			
29a′	−0.97	CO + d_{Co}	10(d_{yz})	2	83	2
20a″	−0.99	CO + d_{Co}	3(p_z); 12(d_{xz}); 3(d_{yz})	2	76	2
28a′	−2.21	NO + d_{Co}	29($d_{x^2-y^2}$)	56	6	8
19a″	−2.22	NO + d_{Co}	2(d_{xz}); 34(d_{yz})	55		9
27a′	−3.22	*i*Pr-DAB (π^*); d_{Co} (π)	12(d_{xy})	10	2	74 (π^*)
			Occupied			
26a′	−4.54	d_{Co} (σ)	2(s); 4(p); 78(d_{z^2})	5	3	5
18a″	−4.75	d_{Co} + ligands	6(p_z); 20(d_{xz}); 29(d_{yz});	19	13	12
25a′	−5.05	d_{Co} (π); Pr-DAB (π^*)	8(p_x); 5(d_{z^2}); 11($d_{x^2-y^2}$); 33(d_{xy})	13	7	19
17a″	−5.53	d_{Co} + NO	57(d_{xz}); 8(d_{yz})	22	2	12
24′	−6.08	d_{Co}	3(p_y); 4(d_{z^2}); 31($d_{x^2-y^2}$); 25(d_{xy})	21	7	7
16a″	−7.18	*i*Pr-DAB (π)	6(d_{xz})			93 (π)

Table 6. Calculated Spin Densities and Isotropic Fermi Contact Coupling Constants (10^{-4} cm^{-1}) for [(Me-DAB)Co(NO)(CO)]$^{\bullet-}$ and Experimental EPR Hyperfine Splitting (hfs) Constants for [(*i*Pr-DAB)Co(NO)(CO)]$^{\bullet-}$

atom	spin density G98/B3LYP	spin density ADF/BP	hfs G98/B3LYP	hfs ADF/BP	hfs exptl
^{53}Co	0.109	−0.009	10.86	−8.29	10.57
^{14}N	0.332	0.265	6.82	3.66	6.08
^{14}N(NO)	0.055	0.144	3.71	3.89	2.06
^{1}H	−0.008	−0.007	−2.75	−3.27	3.83

[a] 1 mT = 9.348×10^{-4} cm^{-1}.

The spin density in [(Me-DAB)Co(NO)(CO)]$^{\bullet-}$ is spread out not only over the R-DAB ligand but also over the Co and N(NO) centers. This is reflected by calculated spin densities at Co and all N centers (Table 6). The optimized geometry of [(R-DAB)Co(NO)(CO)]$^{\bullet-}$ as listed in Table 4 shows the largest changes of structure within the R-DAB ligand; nevertheless, due to the SOMO character the structure of the NO−Co−CO fragment is also influenced in the course of reduction. The calculated hyperfine splittings are listed together with the spin densities in Table 6 and were calculated for the model complex radical [(Me-DAB)Co-(NO)(CO)]$^{\bullet-}$ at optimized geometry. The experimental hyperfine coupling is rather well described by the G98/B3LYP calculation results with basis II; an extended Co basis set including diffusion functions is necessary for an interpretation of the large hyperfine coupling of the Co atom.

In general, the metal hyperfine splitting is particularly sensitive to reproduce due to the crucial influence of core electrons, as is also evident from the large experimental variation observed (Table 1). However, the order of magnitude for $a(^{59}Co)$ agrees with that found for porphyrin radical complexes of nitrosylcobalt.[35] The thus extracted spin distribution with about 85% on R-DAB, 10% on Co, and 5% on NO is in excellent agreement with the other results presented here.

The assignment of the IR frequencies of (*i*Pr-DAB)Co-(NO)(CO) is supported by ADF/BP calculations (Table 7) on the model complex (Me-DAB)Co(NO)(CO). The intense

(35) Kadish, K. M.; Mu, X. H.; Lin, X. Q. *Inorg. Chem.* **1988**, *27*, 1489.

Table 7. ADF/BP Calculated CO and NO Stretching Frequencies ν (cm^{-1}) for (R-DAB)Co(NO)(CO) and $[(R\text{-DAB})Co(NO)(CO)]^{\bullet -}$ [a]

(R-DAB)Co(NO)(CO)		$[(R\text{-DAB})Co(NO)(CO)]^{\bullet -}$		
calcd	exptl	calcd	exptl	assignment
1738	1689	1589	1577	νNO
1954	1942	1851	1868	νCO

[a] R = *i*Pr (exptl), R = Me (calcd).

Table 8. TD-DFT (ADF/BP) Calculated Lowest Singlet Excitation Energies (eV) and Oscillator Strengths for (*i*Pr-DAB)Co(NO)(CO)[a]

state	composition	calcd trans. energy/λ (eV/nm)	osc str	exptl trans. energy/λ (eV/nm)
$^1A'$	97% (26a′ → 27a′)	1.46/849	0.001	n.o.
$^1A'$	64% (25a′ → 27a′) 14%(18a″ → 19a″) 11% (24a′ → 27a′)	2.59/479	0.039	2.27/545
$^1A'$	62%(18a″ → 19a″) 16% (17a″ → 19a″) 14%(24a′ → 27a′)	3.07/404	0.036	2.81/438
$^1A'$	50% (25a′ → 28a′) 8%(25a′ → 27a′) 18% (24a′ → 27a′)	3.31/375	0.022	3.75sh/330sh

[a] λ = wavelength, osc str = oscillator strength, n.o. = not observed, trans. = transition.

feature around 1942 cm^{-1} is assigned to the C−O stretching mode (calculated at 1954 cm^{-1}); the second intense one around 1689 cm^{-1} is assigned to the N−O stretching mode (calculated at 1738 cm^{-1}). The shift of both frequencies to smaller wavenumbers in the course of reduction is also reproduced by the differences of calculated frequencies for CO and NO; the calculations confirm the larger shift for the NO stretching vibration. The CO frequency of the reduced complex measured at 1868 cm^{-1} is calculated at 1851 cm^{-1} while the NO frequency (measured at 1577 cm^{-1}) is calculated at 1589 cm^{-1}.

The TD-DFT calculated lowest singlet excitation energies for (*i*Pr-DAB)Co(NO)(CO) are listed Table 8. After a very low-intensity transition, the first allowed electronic transition calculated at 2.59 eV (479 nm) can be characterized as an $^1A'$ (MLCT) transition. Its largest contribution is the excitation from HOMO − 2, 25a′, into the LUMO, 27a′. The following two allowed transitions are composed from several one-electron excitations involving mainly the two low-lying π* MOs of the coordinated NO group. Therefore, we assign the two detectable bands in the visible and near-UV regions of the complexes to MLCT transitions from cobalt(I−) d orbitals to π*(R-DAB) at longer wavelengths and to π*-(NO) at higher energies. There is even a rather good correspondence of experimental and calculated excitation energies (Table 8). The existence of two different excitations as suggested by rR spectroscopy is thus confirmed by calculations although the contributions from the nitrosyl ligand are not reflected in the rR experiments which could be carried out only for the complexes of the higher substituted R-DAB ligands.

Summary

The results obtained here for three different compounds (R-DAB)Co(NO)(CO) demonstrate a strong effect of the groups R, as is particularly evident from the quite variable reduction potentials and the ^{59}Co hyperfine coupling of the radical anions. While it is not unexpected that the first reduced and lowest MLCT excited states involve the π* MO of the R-DAB ligands, the contributions from the NO ligand are fairly obvious. In the EPR spectra, the lowered *g* values, the detectable and DFT-reproduced ^{14}N(NO) hyperfine coupling, and the decreased ^{14}N(R-DAB) hyperfine splitting are indicative while the additional absorption bands and the stronger shift of ν_{NO} versus ν_{CO} on reduction also point to the theoretically confirmed NO participation. While more robust nitrosylcobalt complexes have found recent interest as NO sensor materials,[36,37] the conceptually simple compounds described herein have allowed a more straightforward assessment of the role of the different acceptor ligands.

Acknowledgment. This work was supported by the Deutsche Forschungsgemeinschaft, Fonds der Chemischen Industrie, and the European Community (Program COST D14). Support of this work from Robert Bosch GmbH (Stuttgart) and from the Ministry of Education of the Czech Republic and the DLR (Bonn) for KONTAKT Project CZE 00/013 is gratefully acknowledged. We also thank Professor J. A. Olabe and Dr. F. Doctorovich (Universidad de Buenos Aires) for valuable discussions.

IC026078T

(36) (a) Shioya, T.; Swager, T. M. *Chem. Commun.* **2002**, 1364. (b) Franz, K. J.; Singh, N.; Lippard, S. J. *Angew. Chem.* **2000**, *112*, 2194; *Angew. Chem., Int. Ed.* **2000**, *39*, 2120.

(37) Weil, J. A.; Bolton, J. R.; Wertz, J. E. *Electron Paramagnetic Resonance*; Wiley: New York, 1994.